



Synthesis and hydrolytic evaluation of acid-labile imine-linked cytotoxic isatin model systems

Lidia Matesic^a, Julie M. Locke^{a,b}, Kara L. Vine^c, Marie Ranson^c, John B. Bremner^a, Danielle Skropeta^{a,*}

^aSchool of Chemistry and Centre for Medicinal Chemistry, University of Wollongong, Wollongong, NSW 2522, Australia

^bIntelligent Polymer Research Institute, University of Wollongong, Wollongong, NSW 2522, Australia

^cSchool of Biological Sciences and Illawarra Health and Medical Research Institute, University of Wollongong, Wollongong, NSW 2522, Australia

ARTICLE INFO

Article history:

Received 28 November 2010

Revised 6 January 2011

Accepted 10 January 2011

Available online 14 January 2011

Keywords:

Isatin

Hydrolysis

Acid-catalysed

Imines

Prodrugs

ABSTRACT

In this study a series of isatin-based, pH-sensitive aryl imine derivatives with differing aromatic substituents and substitution patterns were synthesised and their acid-catalysed hydrolysis evaluated. These derivatives were functionalised at the C3 carbonyl group of a potent *N*-substituted isatin cytotoxin and were stable at physiological pH but readily cleaved at pH 4.5. Observed rates of hydrolysis for the embedded imine-acid moiety were in the order *para*-phenylpropionic acid > phenylacetic acid (*para* > *meta*) > benzoic acid (*meta* > *para*). The ability to fine-tune hydrolysis rates in this way has potential implications for optimising imine linked, tumour targeting cytotoxin–protein conjugates.

© 2011 Elsevier Ltd. All rights reserved.

1. Introduction

A promising strategy for anti-cancer drug delivery involves conjugating a cytotoxin with a tumour targeting protein through an acid-labile linker that is stable at physiological pH.^{1,2} Internalisation at the target tumour site via processes such as receptor mediated endocytosis³ exposes the conjugate to the acidic environment of the endosomes or lysosomes (pH 4.5–6.0), resulting in selective release of the original cytotoxin inside the tumour cell.^{4,5}

Over the years, a wide variety of functional groups have been employed in the development of linkers that are stable at physiological pH (7.4), but cleave at endosomal/lysosomal pH including acid-sensitive hydrazones,^{6–9} *cis*-aconityl groups,¹⁰ trityl groups,^{4,11} orthoesters¹² and *N*-ethoxybenzylimidazoles.¹³ In particular, the antineoplastic anthracyclines doxorubicin and daunorubicin have been conjugated through hydrazone and *cis*-aconityl linkers.^{4,6,10,14,15} The hydrazone linker has, however, been reported to cleave at non-target sites¹⁶ and at pH 7.4,¹⁷ which suggests that this linker may be unstable in the circulatory system. Other less commonly employed acid-labile linkers include acetals,^{18,19} ketals,¹⁹ oximes²⁰ and imines.^{21,22}

The imine group as part of a selective acid-sensitive linker to tumour targeting proteins was of potential interest in our work on

potent isatin-based cytotoxins.^{23–25} The cytotoxicities against U937 lymphoma cells of these compounds, together with that of isatin itself for comparison purposes, is shown in Figure 1.

The most potent isatin-based cytotoxins we have developed are derivatised on both the aromatic ring and via *N*-substitution.^{23–25} Therefore the aim of this study was to generate a pH-sensitive linker that did not interfere with these areas of the molecule, but instead capitalised on the available carbonyl group at C-3, which is present in all of our isatin-derived cytotoxins. This could be achieved using an imine linker. Although imine linkers are not widely employed in drug delivery,²⁶ they have gained attention in recent years with several studies showing that aromatic imines with extended π – π conjugation are stable at physiological pH, while readily hydrolysing in mildly acidic solutions (e.g., pH 4.5–6.8).^{27–31}

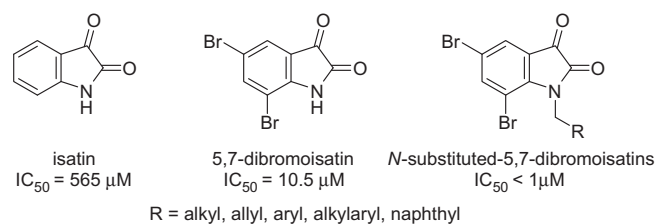
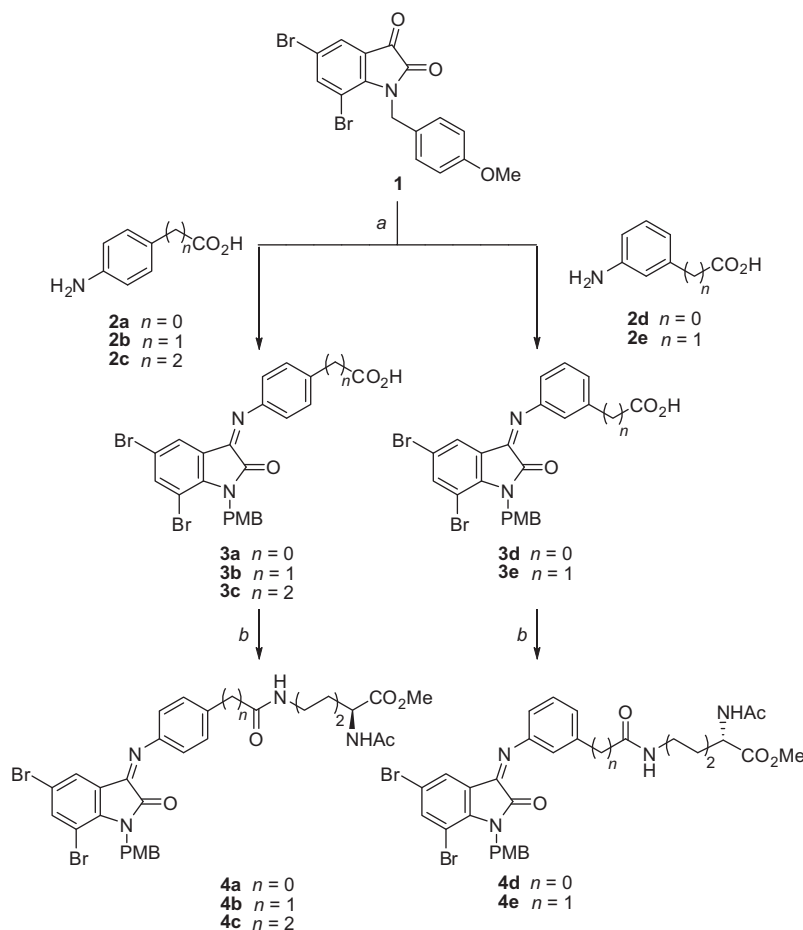


Figure 1. Cytotoxic activity of isatin and its derivatives against the human monocyte-like histiocytic lymphoma U937 cell line.^{23–25}

* Corresponding author. Tel.: +61 2 42214360; fax: +61 2 4221 4287.

E-mail addresses: skropeta@uowmail.edu.au, skropeta@uow.edu.au (D. Skropeta).



Scheme 1. Reagents and conditions: (a) EtOH, AcOH (cat.), reflux, 1.5 h, 18–71%; (b) DCC, HOBt, DIPEA, Ac-Lys-OMe-HCl, CH₂Cl₂, rt, 24 h, 41–82% (PMB = *para*-methoxybenzyl).

Thus, reaction of our isatin-derived cytotoxins (e.g., **1**) with a bifunctional linker such as the anilino carboxylic acids **2a–e**, would give the aryl imine linked cytotoxins **3a–e** shown in Scheme 1. These compounds, with a free carboxylic acid available for potential coupling via amide formation to the exposed lysine residues on a suitable tumour targeting protein, would be expected to be stabilised by extended resonance delocalisation. Furthermore, acid-catalysed hydrolysis of the imine-linked cytotoxins should result in selective release of the original isatin cytotoxin (**1**). This would be an improvement over some of the existing pH-sensitive bioconjugation strategies, where hydrolysis of the linker generates a modified derivative of lower potency than the original cytotoxin.¹³

The benchmark chemical studies required to establish the imine group as a feasible cytotoxin linking option for isatins, together with related model work, are now presented in this paper. In particular, we have prepared the aryl imine derivatives (**3a–e**) of the cytotoxic isatin (**1**) via reaction with the bifunctional, acid–amine linkers (**2a–e**) (Scheme 1). The carboxylic moieties in **3a–e** were then used to react with the ϵ -amino group of an α -*N,C*-protected lysine derivative to afford the amides (**4a–e**), as a preliminary model of such reactions with protein based lysine residues. The hydrolytic efficiencies of the imines (**3a–e**) and amides (**4a–e**) were evaluated using UV–vis spectrophotometry. Herein, we report the first instance of the pH-dependent selective release of a potent *N*-alkylisatin derived cytotoxin through the acid-catalysed hydrolysis of an aryl imine linker.

2. Results

2.1. Synthesis

The five novel aryl imine derivatives **3a–e** were readily prepared by the acid-catalysed reaction of the brominated cytotoxin, *N*-*para*-methoxybenzylisatin cytotoxin (**1**), with a range of commercially available anilino carboxylic acids (**2a–e**), differing in terms of their aromatic substitution patterns and by the length of the linker between the aromatic ring and the carboxylic acid moiety (Scheme 1). For this study, *para*- and *meta*-benzoic (**2a**, **2d**), *para*- and *meta*-phenylacetic (**2b**, **2e**) and *para*-phenylpropionic (**2c**) anilino carboxylic acids were selected. The isatin **1** and the appropriate acids **2a–e** were then heated at reflux in MeOH or EtOH together with a catalytic amount of AcOH for 1.5 h to yield the imines **3a–e**. Reactions in this study proceeded in moderate to high yield, with the phenylacetic and phenylpropionic acids (e.g., **3b**, **3c**, **3e**) affording higher yields. Imines **3b–e** were produced in higher yields with the higher boiling EtOH rather than MeOH, while **3a** was the only imine to favour MeOH over EtOH. Lack of the AcOH catalyst led to a decrease in chemical yield. There was also no evidence, as seen by ¹H NMR spectroscopy, (DMSO-*d*₆) of self-cleavage of the imines **3a–e** to the free isatin **1**.

Imines **3a–e** were obtained as mixtures of *E* and *Z* isomers about the imine bond and could not be separated by either thin-layer chromatography or HPLC, as has been reported for other 3-arylimino-2-indolinones.³² The ¹H NMR spectra of the imines **3a–e** in DMSO-*d*₆, revealed that most compounds (**3a–d**) were synthesised

as approximately 1:1 mixtures of *E/Z* isomers, apart from the *meta*-phenylacetic imine (**3e**) where the *E* isomer was favoured over the *Z* isomer in an approximate 2:1 ratio. The *E* stereochemistry was assigned to a particular isomer based on the following: the signal from H4 (on the isatin core) of the *E* isomer in the ¹H NMR spectrum was shifted upfield 1.2–1.4 ppm relative to the H4 signals of the *Z* isomer and the parent compound **1**, presumably due to shielding by the ring current on the iminophenyl ring. The isomeric ratios of each compound were therefore determined by comparing the size of the integrals from the H4 signals of the *E* and *Z* isomers, as has been described previously by our group for a related series of compounds.²³ Although some 2-indolinones containing a substituent at C-3 have been described as predominantly *E* isomers,³³ elsewhere it has been reported that the *E* and *Z* isomers of 3-imino-2-indolinones interconvert rapidly in solution at room temperature and that the ratio of isomers is solvent dependent.³² The imines **3b–e** were formed in good yields (56–71%), whereas **3a** was obtained in only 18% yield. This presumably results from the reduced nucleophilicity of the amino moiety in **3a**, relative to that in **3b–e**, due to the strong electron withdrawing effect of the *para*-substituted carboxyl group.

The imino acids (**3a–e**) were then selectively coupled to the protected lysine derivative Ac-Lys-OMe under standard carbodiimide coupling procedures,^{34,35} to give the desired novel imine–lysine model conjugates **4a–e** in good to excellent yields (Scheme 1). Once again, the ¹H NMR spectra (CDCl₃) of the isatin–lysine series (**4a–e**) revealed that most compounds (**4a–d**) were synthesised as approximately 1:1 mixtures of *E/Z* isomers, apart from the *meta*-phenylacetic analogue (**4e**) where the *Z* isomer was favoured over the *E* isomer in an approximate 2:1 ratio, the reverse ratio to that observed for the precursor imine **3e**. This may, however, be due to the change in NMR solvent from DMSO-*d*₆ with **3e** to CDCl₃ with **4e**, as has been observed for other imines.³² All of the imines (**3a–e**, **4a–e**) were fully characterised by ¹H and ¹³C NMR spectroscopy and mass spectrometry.

2.2. Hydrolysis studies

The rate of acid-catalysed hydrolysis in the imino acids **3a–e** as a function of imine absorbance at $\lambda = 435$ nm over time is shown in Figure 2A (middle panel). Analysis of the hydrolysis kinetics conducted at pH 4.5 (37 °C) indicated an exponential first order decay process as evidenced by the $\ln(A/A_0)$ versus time plots (Fig. 2A, bottom panel), which showed a linear relationship at the initial reaction times. The first order rate constants, *k*, determined by non-linear regression, ranged from 0.95 to $3.99 \times 10^{-2} \text{ min}^{-1}$ (Table 1), which is comparable to those reported in an earlier study by Kalavska et al. of acid-catalysed hydrolysis of some substituted derivatives of 3-phenyliminoxindole at pH 2.0–5.0.³⁶ It should be noted, however, that these derivatives differ from those herein in that they are neither *N*-alkylated nor halogenated on the isatin aromatic ring, and bear different imino aryl substituents at the C3 position. The fastest hydrolysis rate, as indicated by the largest *k* value, was observed for the *para*-phenylpropionic acid derivative **3c**, with a half-life of 17.4 min. Conversely, the smallest *k* value was found for the *para*-benzoic acid derivative **3a**, which displayed a fourfold greater half-life of 72.6 min. As discussed earlier, this compound had the lowest yield of imine formation (18%). In contrast, imines which demonstrated efficient hydrolytic release (**3b**, **3d**, and **3e**) were formed in good yields (>68%). These three imino acid derivatives did not show any significant differences to one another in their hydrolysis rates, as judged by one-way ANOVA, and displayed half-lives ranging from 24.3 to 29.7 min. Although compounds **3a–e** were monitored kinetically over a 240 min period, results are only displayed over a 60 min period as all derivatives reached a plateau in terms of hydrolysis in less than 240 min. No

hydrolysis was detected for the derivatives **3a–e** when maintained at physiological pH (7.4) in 1 M HEPES buffer at 37 °C over a 240 min period (the first 60 min shown in Fig. 2A, top panel).

A similar trend in the rate of hydrolysis was obtained for the imino lysine conjugates **4a–e** (Fig. 2B) with first order rate constants, *k*, ranging from 0.81 to $4.07 \times 10^{-2} \text{ min}^{-1}$ (Table 1). Again, the fastest hydrolysis rate was observed for the *para*-phenylpropionic acid derivative **4c** with a half-life of 17.0 min, and the lowest hydrolysis rate was found for the *para*-benzoic acid derivative **4a**, which had a fivefold greater half-life of 85.2 min. In this case, the hydrolysis rates of all but **4d** versus **4e** were found to be significantly different from one another, as judged by one-way ANOVA, with the *para*-phenylacetic acid derivative **4b** significantly faster than both **4d** and **4e**, with half-lives of 34.1 and 33.0 min, respectively, compared to 23.0 min for **4b**. As for the imino acids **3a–e**, no hydrolysis was detected for the imino lysine derivatives **4a–e** when maintained at physiological pH (7.4) in 1 M HEPES buffer at 37 °C over a 240 min period (Figure 2B, top panel).

Hydrolysis of the various derivatives was found to depend on the aromatic substitution pattern and linker length and was not influenced by whether the derivatives were in the imino acid or imino lysine form. This can be seen by comparing the hydrolysis rates of each pair of derivatives (e.g., **3a**: $k = 0.95 \times 10^{-2} \text{ min}^{-1}$ vs **4a**: $k = 0.81 \times 10^{-2} \text{ min}^{-1}$), which showed no significant difference as judged by one-way ANOVA (see Supplementary data).

In addition to the hydrolysis experiments conducted at physiological temperatures (37 °C), selected hydrolyses for **3a**, **3b** and **3d** were also conducted at ambient temperature. As expected, the rates of hydrolysis at pH 4.5 were significantly lower at 23 °C compared to those conducted at 37 °C, while no hydrolysis was detected at physiological pH at either 23 °C or 37 °C (see Supplementary data).

3. Discussion and conclusion

We have reacted various anilino carboxylic acids (**2a–e**) with the potent cytotoxin *para*-methoxybenzylisatin (**1**) to generate a series of aryl imine derivatives (**3a–e**, Scheme 1) with differing aromatic substitution patterns and linker length. Alkyl imine derivatives are known to hydrolyse at physiological pH, however, aryl imines are significantly more stable and have found recent potential application as pH-sensitive linkers in drug delivery.^{27–31} Accordingly, the aryl imines we prepared were all found to be stable at physiological pH but readily cleaved at reduced pH. Furthermore, in order to model the conjugation of these acid-labile derivatives to the lysine residues of a tumour-targeting protein, the aryl imines **3a–e** were coupled via their free carboxylic acids to a protected lysine amino acid residue to produce a novel series of aryl imine–lysine conjugates **4a–e**. These were all found to be stable for an extended period at pH 7.4 but readily cleaved in aqueous acidic solutions at physiological temperature, with half-lives ranging from 17.0 to 85.2 min, consistent with those reported recently for the acid-catalysed hydrolysis of other aryl imines.³¹

The rates of acid-catalysed hydrolysis of both the imino acids **3a–e** and imino lysines **4a–e**, followed the expected trend, with the *para*-phenyl propionic acid derivatives (**3c** and **4c**) displaying the fastest hydrolysis rates, and the *para*-benzoic acid derivatives (**3a** and **4a**) displaying the lowest rates.

Acid-catalysed hydrolysis of imines involves the protonation of the imine to give an iminium species, which undergoes nucleophilic attack by water. This gives an unstable hemiaminal intermediate, which upon protonation of the amine nitrogen, readily collapses to the protonated ketone and free amine, with subsequent proton loss furnishing the ketone.³⁷ The crucial first step in the mechanism, imine protonation, is largely dependent on the basicity of the imine. In derivatives **3a** and **4a**, the electron-withdrawing carbonyl group directly attached to the *para*-position on the phenyl

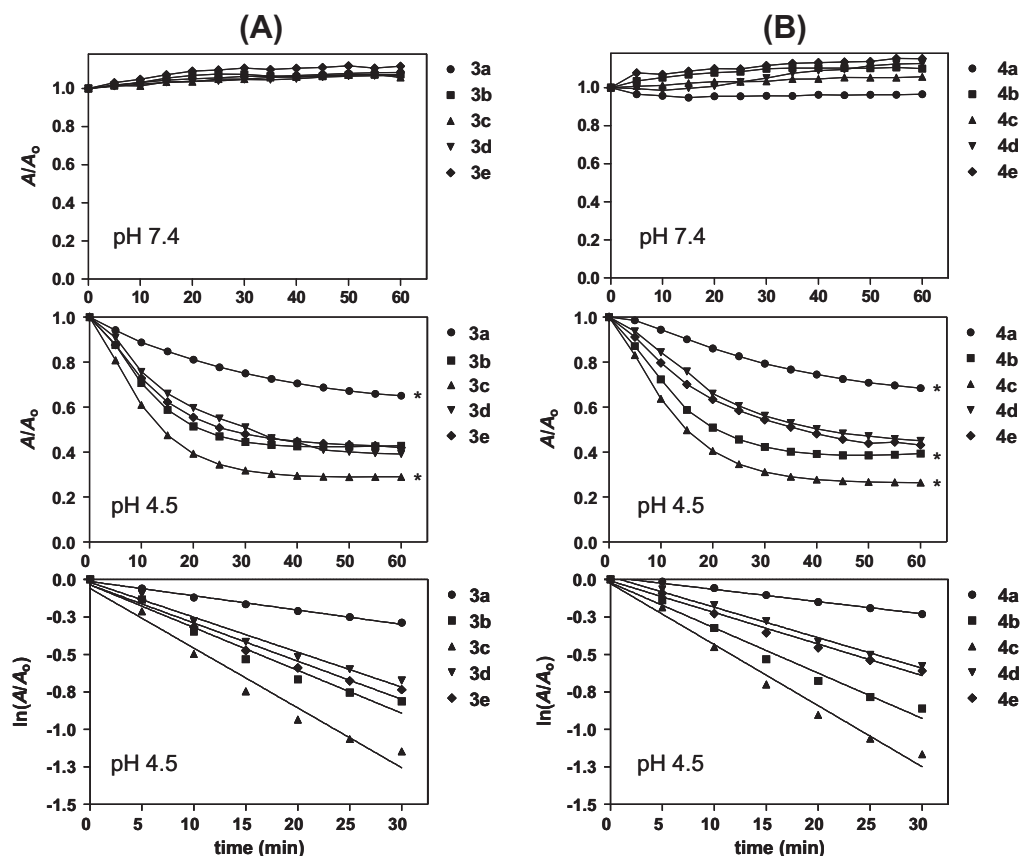


Figure 2. Rates of hydrolysis expressed as a function of absorbance (A/A_0) over time (pH 7.4 top panel and pH 4.5 middle panel) and the natural log of absorbance (A/A_0) over time (bottom panel, pH 4.5), measured at 435 nm in 1 M sodium acetate buffer at 37 °C for (A, middle panel): the imino acid derivatives **3a–e** (* $P < 0.05$ for **3a** vs **3b–e**; **3c** vs **3b**, **3d** and **3e**); and (B, middle panel): the imino lysine derivatives **4a–e** (* $P < 0.05$ for **4a** vs **4b–e**; **4b** vs **4c–e**; **4c** vs **4d** and **4e**).

Table 1

Rate constants (k) and half-lives ($t_{1/2}$) for the hydrolysis of the imino acids **3a–e** and the imino lysines **4a–e** at pH 4.5^a

Imine	n	Substitution pattern	k (min^{-1})	$t_{1/2}$ (min)
$R = \text{OH}$				
3a	0	<i>para</i> -	$0.95 \pm 0.0 \times 10^{-2}$	72.6
3b	1	<i>para</i> -	$2.85 \pm 0.2 \times 10^{-2}$	24.3
3c	2	<i>para</i> -	$3.99 \pm 0.3 \times 10^{-2}$	17.4
3d	0	<i>meta</i> -	$2.33 \pm 0.2 \times 10^{-2}$	29.7
3e	1	<i>meta</i> -	$2.55 \pm 0.2 \times 10^{-2}$	27.2
$R = (\text{CH}_2)_4\text{CH}(\text{NHAc})\text{CO}_2\text{Me}$				
4a	0	<i>para</i> -	$0.81 \pm 0.0 \times 10^{-2}$	85.2
4b	1	<i>para</i> -	$3.02 \pm 0.2 \times 10^{-2}$	23.0
4c	2	<i>para</i> -	$4.07 \pm 0.2 \times 10^{-2}$	17.0
4d	0	<i>meta</i> -	$2.03 \pm 0.1 \times 10^{-2}$	34.1
4e	1	<i>meta</i> -	$2.10 \pm 0.1 \times 10^{-2}$	33.0

^a Rates of hydrolysis were measured at 37 °C in 1 M sodium acetate buffer at pH 4.5 using UV spectrophotometry ($\lambda = 435$ nm). See Section 4 for further details.

ring, will reduce the relative basicity of the imine nitrogen through extended conjugation (Fig. 3), leading to lower rates of hydrolysis as observed. Conversely, for the homologous **3b** and **4b** derivatives, conjugation with the acid or amide carbonyl is disrupted leading to greater availability of the imine nitrogen lone pair of electrons for protonation. Furthermore, hyperconjugation³⁸ in these neutral

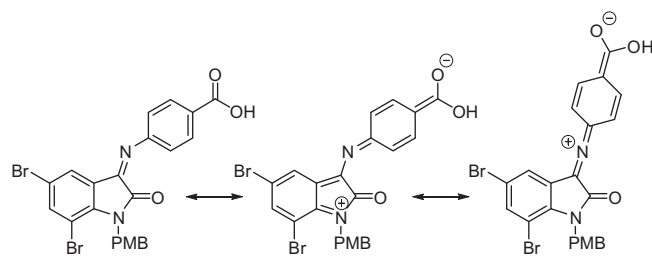


Figure 3. Resonance contributors of the imine **3a** showing extended π delocalisation.

derivatives could be involved in increasing electron density on the carbon adjacent to the imine nitrogen and thereby its relative basicity. This hyperconjugative interaction could be more significant with the *para*-propionic derivatives **3c** and **4c**, with the counter delocalising effect of the carbonyl group adjacent to the negative charge on the Ar-CH carbon being removed. The hyperconjugative effects associated with these groups in the *meta*-position would not be expected to have a marked effect on the imine basicity.

Our results are consistent with those from complementary studies on 3-phenyliminoxindole derivatives, where it was found that electron-donating groups at the *para*-position of the aryl ring enhanced the rates of acid-catalysed hydrolysis.³⁶ Conversely, the incorporation of electron-withdrawing groups on a series of related aryl imines were found to have a stabilising effect at physiological pH.³¹ Thus, it is expected that the incorporation of other

electron donating or withdrawing groups would allow for more tunable hydrolysis rates of imine-based compounds.

Adjusting the linker length was more important in determining hydrolysis rates in the *para*-series compared to the *meta*-series. For both the *para*-substituted carboxylic acid derivatives **3a–c** and the lysine derivatives **4a–c**, lengthening the linker resulted in a significant increase in the hydrolysis rate. However, the two *meta*-substituted derivatives in each series (**3b,d** and **4b,d**), showed no significant difference in their hydrolysis rates. Overall, it appears that electronic effects such as the presence or absence of a conjugated electron-withdrawing group may play a larger role in determining the hydrolysis rate than extending the linker.

In this study we chose the *para*-methoxybenzylisatin (**1**), which has an IC₅₀ value of 1.83 μM²⁴ against the human monocyte-like histiocytic lymphoma U937 cell line, as our starting cytotoxin due to its ready synthetic availability and structural simplicity, which facilitates product characterisation via NMR spectroscopy. While **1** is less active than our most promising cytotoxins (IC₅₀ = 1.83 μM vs <1 μM, respectively),²⁴ the bioconjugation strategy presented here should apply equally well to any of the *N*-substituted isatin derived cytotoxins we have developed, all of which contain an available carbonyl at C-3. This strategy is also potentially applicable to the bioconjugation of well known anti-cancer agents such as epipodophyllotoxin, camptothecin and colchicine to enhance their effectiveness even further.^{39,40} In conclusion, a series of novel aryl imine linked isatins (**3a–e**), which could potentially be coupled to the lysine residues of a tumour targeting protein via standard peptide coupling techniques, were synthesised from the *N*-substituted isatin-derived cytotoxin (**1**). Compounds (**3a–e**) and the model lysine coupled derivatives (**4a–e**) are stable at physiological pH but readily undergo acid-catalysed imine hydrolysis at pH 4.5. Furthermore, the rate of hydrolysis can be fine-tuned through the use of different aromatic substitution patterns on the anilino carboxylic acids (**2a–e**) and by adjusting the linker length. Based on the strategy described here, work is currently underway on the development of potential imine-linked *N*-alkylisatin based tumour targeting cytotoxin-protein conjugates.

4. Experimental

4.1. Synthesis

All chemicals were purchased from Sigma–Aldrich Chemical Co. (St. Louis, MO, USA), BDH Laboratory Supplies (Poole, England) or Bachem (AusPep, Parkville, Australia) and used as supplied. Flash column chromatography⁴¹ was performed on Silica Gel 60 (230–400 mesh). Thin layer chromatography (TLC) on aluminium backed sheets of Merck Silica Gel 60 F₂₅₄ plates were employed to monitor the progress of chemical reactions. Preparative TLC was performed on 20 × 20 cm plates. Solvent ratios are v/v and solvents were removed by rotary evaporation in vacuo. IR spectra were obtained on a Nicolet Avatar 360 FT-IR spectrometer. NMR spectra were acquired on a Varian Inova 500 spectrometer, where the proton (¹H) and carbon (¹³C) were obtained at 500 and 126 MHz, respectively. All spectra were obtained with a probe temperature of 298 K. Hydrogen and carbon assignments were also made using gradient correlation spectroscopy (gCOSY), gradient heteronuclear single quantum correlation (gHSQC) and gradient heteronuclear multiple bond correlation (gHMBC) spectroscopic techniques. Low resolution electrospray ionisation mass spectra (ESI) were obtained using a Waters Platform LCZ spectrometer and high resolution ESI spectra (HRMS) on a Waters Q-TOF Ultima spectrometer. Melting points were obtained using a Reichert melting point apparatus and are uncorrected.

4.1.1. General procedure for the synthesis of the imines (**3a–e**)

Activated 3 Å sieves (1 g per 100 mg of **1**), the isatin **1** (1 equiv) and EtOH (7.5 mL per 100 mg of **1**) (MeOH was used for **3a**) were sonicated for 10 min. The acid (**2a–e**, 1 equiv) was added and the mixture sonicated for a further 5 min before the addition of glacial AcOH (0.2 mL per 100 mg of **1**). The reaction mixture was heated at reflux for 1.5 h, the sieves were filtered and the solution was evaporated. The resulting solid was purified by column chromatography on silica gel using a CHCl₃/MeOH gradient of 100:0 to 95:5 to yield isatins **3a–e**.

4.1.1.1. (*E* and *Z*)-4-[5,7-Dibromo-1-(4-methoxybenzyl)-2-oxoindolin-3-ylideneamino]benzoic acid (**3a**).

Orange powder (46.5 mg, 18%); mixture of *E* and *Z* isomers (*E/Z* 48:52); mp 250–252 °C; R_f 0.26 (silica, DCM); IR ν_{max} 2955 (COOH), 1696 (CO), 1598, 1515, 1446, 1248, 1143, 863, 810 cm⁻¹. δ_H (500 MHz; DMSO-*d*₆): 3.71 (s, 3H), 3.73 (s, 3H), 5.12 (s, 2H), 5.30 (s, 2H), 6.44 (s, 1H), 6.86 (d, *J* = 8.0 Hz, 2H), 6.90 (d, *J* = 8.0 Hz, 2H), 7.13 (d, *J* = 7.5 Hz, 4H), 7.18 (d, *J* = 8.0 Hz, 2H), 7.25 (d, *J* = 8.0 Hz, 2H), 7.84 (s, 1H), 7.87 (s, 1H), 7.91 (d, *J* = 8.5 Hz, 2H), 7.93 (s, 1H), 8.08 (d, *J* = 8.0 Hz, 2H); δ_C (126 MHz; DMSO-*d*₆): 44.0, 44.5, 55.6, 55.7, 104.2, 104.8, 113.2, 114.6,[‡] 114.6,[‡] 114.9, 116.1, 117.6,[‡] 119.5,[‡] 120.6, 125.5, 126.3, 127.7,[‡] 128.2,[‡] 128.2,[‡] 129.3, 129.4,[‡] 130.6,[‡] 131.9, 141.1, 141.3, 143.3, 144.5, 151.1, 152.4, 153.4, 154.0, 158.1, 159.1,[‡] 163.5, 167.6, 167.8. MS (ESI-) *m/z*: 541; 543; 545 [M–H]⁻; ⁷⁹Br⁷⁹Br; ⁷⁹Br⁸¹Br; ⁸¹Br⁸¹Br; HRMS (ESI-) *m/z*: calcd for C₂₃H₁₅N₂O₄⁷⁹Br⁷⁹Br: 540.9399 [M–H]⁻; found: 540.9496 [M–H]⁻.

4.1.1.2. (*E* and *Z*)-2-{4-[5,7-Dibromo-1-(4-methoxybenzyl)-2-oxoindolin-3-ylideneamino]phenyl}acetic acid (**3b**).

Red crystals (356 mg, 68%); mixture of *E* and *Z* isomers (*E/Z* 58:42); mp 151–153 °C; R_f 0.40 (silica, DCM/MeOH 9:1); IR ν_{max} 2935 (COOH), 1708 (CO), 1516, 1445, 1309, 1247, 1142, 802, 753 cm⁻¹. δ_H (500 MHz; DMSO-*d*₆): 3.57 (s, 2H), 3.65 (s, 2H), 3.71 (s, 3H), 3.73 (s, 3H), 5.14 (s, 2H), 5.30 (s, 2H), 6.60 (d, *J* = 1.5 Hz, 1H), 6.87 (d, *J* = 9.0 Hz, 2H), 6.90 (d, *J* = 9.0 Hz, 2H), 7.00 (d, *J* = 8.5 Hz, 2H), 7.13 (d, *J* = 8.5 Hz, 2H), 7.17 (d, *J* = 8.0 Hz, 2H), 7.24 (t, *J* = 7.5 Hz, 4H), 7.41 (d, *J* = 8.5 Hz, 2H), 7.81 (d, *J* = 2.0 Hz, 2H), 7.89 (d, *J* = 2.0 Hz, 1H); δ_C (126 MHz; DMSO-*d*₆): 44.0, 44.6, 55.8,[‡] 104.1, 104.8, 112.5, 114.5,[‡] 114.7,[‡] 115.0, 116.1, 117.8,[‡] 120.7,[‡] 121.1,[‡] 125.1, 127.0, 127.6, 128.2,[‡] 128.3,[‡] 129.5, 130.1, 130.5,[‡] 131.5,[‡] 133.5, 133.7, 141.1, 142.8, 144.4, 146.8, 148.0, 148.9, 158.2, 159.1,[‡] 163.8, 173.5.[‡] MS (ESI+) *m/z*: 557; 559; 561 [MH]⁺; ⁷⁹Br⁷⁹Br; ⁷⁹Br⁸¹Br; ⁸¹Br⁸¹Br; HRMS (ESI+) *m/z*: calcd for C₂₄H₁₉N₂O₄⁷⁹Br⁸¹Br: 558.9692 [MH]⁺; found 558.9678 [MH]⁺.

4.1.1.3. (*E* and *Z*)-3-{4-[5,7-Dibromo-1-(4-methoxybenzyl)-2-oxoindolin-3-ylideneamino]phenyl}propanoic acid (**3c**).

Orange/red crystals (384 mg, 71%); mixture of *E* and *Z* isomers (*E/Z* 55:45); mp 79–81 °C; R_f 0.43 (silica, DCM/MeOH 9:1); IR ν_{max} 2986 (COOH), 1718 (CO), 1514, 1445, 1320, 1247, 1140, 848 cm⁻¹. δ_H (500 MHz; DMSO-*d*₆): 2.55 (t, *J* = 7.5 Hz, 2H), 2.56 (t, *J* = 8.0 Hz, 2H), 2.83 (t, *J* = 7.5 Hz, 2H), 2.89 (t, *J* = 7.5 Hz, 2H), 3.71 (s, 3H), 3.73 (s, 3H), 5.15 (s, 2H), 5.29 (s, 2H), 6.54 (s, 1H), 6.86 (d, *J* = 8.0 Hz, 2H), 6.90 (d, *J* = 7.5 Hz, 2H), 6.96 (d, *J* = 7.5 Hz, 2H), 7.13 (d, *J* = 8.0 Hz, 2H), 7.18 (d, *J* = 8.0 Hz, 2H), 7.22–7.24 (m, 4H), 7.38 (d, *J* = 8.0 Hz, 2H), 7.80 (m, 2H), 7.88 (s, 1H); δ_C (126 MHz; DMSO-*d*₆): 30.7, 30.8, 36.1, 36.5, 44.0, 44.5, 55.7, 55.8, 104.0, 104.7, 114.6,[‡] 114.6,[‡] 114.9, 116.0, 117.8,[‡] 120.6,[‡] 121.5, 124.9, 127.0, 127.5, 128.1,[‡] 128.3,[‡] 128.8,[‡] 129.4, 129.5, 130.2,[‡] 139.5, 140.0, 140.4, 140.9, 142.6, 144.2, 146.4, 148.4, 149.8, 152.3, 158.0, 159.0, 159.1, 163.7, 174.5.[‡] MS (ESI-) *m/z*: 569; 571; 573

[‡] Coincident peaks.

[†] Carboxylic acid proton not detected.

[M–H][−]; ⁷⁹Br⁷⁹Br; ⁷⁹Br⁸¹Br; ⁸¹Br⁸¹Br; HRMS (ESI-) *m/z*: calcd for C₂₄H₁₉N₂O₂⁷⁹Br⁸¹Br: 526.9799 [M–CO₂H][−]; found 526.9722 [M–CO₂H][−].

4.1.1.4. (E and Z)-3-[5,7-Dibromo-1-(4-methoxybenzyl)-2-oxoindolin-3-ylideneamino]benzoic acid (3d). Orange powder (144 mg, 56%); mixture of *E* and *Z* isomers (*E/Z* 49:51); mp 229–231 °C; *R*_f 0.37 (silica, DCM/MeOH 9:1); IR *v*_{max} 2950 (COOH), 1719 (CO), 1698, 1515, 1449, 1297, 1250, 1141, 812, 768 cm^{−1}. δ_{H} (500 MHz; DMSO-*d*₆): 3.71 (s, 3H), 3.73 (s, 3H), 5.13 (s, 2H), 5.30 (s, 2H), 6.41 (s, 1H), 6.86 (d, *J* = 8.5 Hz, 2H), 6.90 (d, *J* = 9.0 Hz, 2H), 7.17 (d, *J* = 8.0 Hz, 2H), 7.25 (d, *J* = 8.5 Hz, 2H), 7.29 (d, *J* = 7.5 Hz, 1H), 7.34 (d, *J* = 8.0 Hz, 1H), 7.47 (t, *J* = 8.0 Hz, 1H), 7.59 (s, 1H), 7.65 (t, *J* = 8.0 Hz, 2H), 7.74 (d, *J* = 7.5 Hz, 1H), 7.82 (s, 1H), 7.85 (s, 1H), 7.88 (d, *J* = 7.5 Hz, 1H), 7.91 (s, 1H), 13.13 (br s, 2H). δ_{C} (126 MHz; DMSO-*d*₆): δ 44.0, 44.5, 55.7, 104.1, 104.7, 114.6, 114.6, 114.8, 116.0, 118.3, 120.7, 120.9, 122.0, 124.5, 125.2, 126.6, 126.8, 126.9, 127.5, 128.1, 128.2, 129.3, 129.4, 130.8, 132.1, 140.8, 141.0, 143.1, 144.5, 149.1, 150.4, 151.2, 153.0, 158.1, 159.0, 163.6, 167.5, 167.8. MS (ESI-) *m/z*: 541; 543; 545 [M–H][−]; ⁷⁹Br⁷⁹Br; ⁷⁹Br⁸¹Br; ⁸¹Br⁸¹Br; HRMS (ESI-) *m/z*: calcd for C₂₃H₁₅N₂O₄⁷⁹Br⁷⁹Br: 540.9399 [M–H][−]; found 540.9424 [M–H][−].

4.1.1.5. (E and Z)-2-{3-[5,7-Dibromo-1-(4-methoxybenzyl)-2-oxoindolin-3-ylideneamino]phenyl}acetic acid (3e). Red powder (187 mg, 71%); mixture of *E* and *Z* isomers (*E/Z* 67:33); mp 182–184 °C; *R*_f 0.33 (silica, DCM/MeOH 9:1); IR *v*_{max} 2944 (COOH), 1719 (CO), 1698, 1515, 1449, 1297, 1250, 1141, 812, 768 cm^{−1}. δ_{H} (500 MHz; DMSO-*d*₆): δ 3.56 (s, 2H), 3.63 (s, 2H), 3.71 (s, 3H), 3.73 (s, 3H), 5.14 (s, 2H), 5.30 (s, 2H), 6.61 (s, 1H), 6.86 (d, *J* = 8.0 Hz, 2H), 6.90 (d, *J* = 8.5 Hz, 2H), 6.94 (d, *J* = 8.5 Hz, 1H), 7.04 (s, 1H), 7.08 (d, *J* = 7.5 Hz, 1H), 7.17 (d, *J* = 8.5 Hz, 2H), 7.20 (d, *J* = 8.0 Hz, 2H), 7.23 (d, *J* = 8.0 Hz, 2H), 7.28 (t, *J* = 7.5 Hz, 1H), 7.46 (t, *J* = 7.5 Hz, 1H), 7.78–7.80 (m, 2H), 7.90 (s, 1H), 8.00 (s, 1H). δ_{C} (126 MHz; DMSO-*d*₆): 41.2, 41.6, 43.9, 44.5, 55.7, 104.1, 104.6, 114.5, 114.6, 115.1, 115.4, 115.9, 116.0, 117.4, 118.6, 118.7, 120.6, 121.8, 125.0, 126.8, 126.9, 127.3, 127.5, 127.8, 128.1, 128.2, 128.8, 129.3, 129.4, 130.3, 140.6, 141.0, 142.8, 144.3, 148.6, 150.3, 152.3, 158.0, 159.0, 163.7, 173.0, 173.1. MS (ESI-) *m/z*: 555; 557; 559 [M–H][−]; ⁷⁹Br⁷⁹Br; ⁷⁹Br⁸¹Br; ⁸¹Br⁸¹Br; HRMS (ESI-) *m/z*: calcd for C₂₄H₁₇N₂O₄⁷⁹Br⁸¹Br: 556.9535 [M–H][−]; found 556.9568 [M–H][−].

4.1.2. General procedure for the synthesis of the imine–lysine conjugates (4a–e)

The isatin imine (**3a–e**, 1 equiv) was dissolved in dry DCM (1 mL per 30 mg of imine) with the aid of sonication. On ice, 1-hydroxybenzotriazole hydrate (HOBT) (1 equiv) was added, followed by *N,N*-dicyclohexylcarbodiimide (DCC) (1 equiv), *N,N*-diisopropylethylamine (DIPEA) (1.1 equiv) and (*S*)-*N* α -acetyl-lysine methyl ester hydrochloride (Ac-Lys-OMe·HCl) (1 equiv). The reaction mixture was warmed to rt and stirred for 24 h. The precipitate was removed by filtration and the filtrate evaporated. The resulting solid was purified by column chromatography on silica gel using a CHCl₃/MeOH gradient of 100:0 to 95:5 to yield the imine–lysine conjugate **4a–e**.

4.1.2.1. Methyl (S,E and S,Z)-2-acetamido-6-{4-[5,7-dibromo-1-(4-methoxybenzyl)-2-oxoindolin-3-ylideneamino]benzamido}hexanoate (4a). Orange crystals (18.7 mg, 50%); mixture of *E* and *Z* isomers (*E/Z* 53:47); mp 165–167 °C; *R*_f 0.41 (silica, CHCl₃/MeOH 95:5). δ_{H} (500 MHz; CDCl₃): 1.39–1.89 (m, 12H), 2.00 (s, 6H), 3.42–3.53 (m, 4H), 3.73 (s, 3H), 3.75 (s, 3H), 3.77 (s, 3H), 3.79 (s, 3H), 4.59–4.64 (m, 2H), 5.24 (s, 2H), 5.44 (s, 2H), 6.23 (dd, *J* = 7.0, 15 Hz, 2H), 6.33 (br s, 1H), 6.51 (br s, 1H), 6.77

(s, 1H), 6.82 (d, *J* = 8.5 Hz, 2H), 6.86 (d, *J* = 8.5 Hz, 2H), 7.03 (d, *J* = 8.5 Hz, 2H), 7.06 (d, *J* = 8.5 Hz, 2H), 7.15 (d, *J* = 8.5 Hz, 2H), 7.22 (d, *J* = 8.0 Hz, 2H), 7.61 (s, 1H), 7.72 (s, 1H), 7.81 (d, *J* = 7.5 Hz, 2H), 7.84 (s, 1H), 7.96 (d, *J* = 8.5 Hz, 2H). δ_{C} (126 MHz; CDCl₃): 22.5, 22.6, 23.4, 28.7, 29.1, 32.2, 32.5, 39.5, 39.7, 44.0, 44.6, 51.9, 52.1, 52.7, 55.5, 104.0, 104.8, 111.4, 114.4, 114.4, 115.9, 116.8, 117.4, 119.4, 119.6, 120.6, 125.8, 127.9, 128.2, 128.3, 128.4, 129.1, 132.1, 133.2, 141.5, 142.1, 142.5, 144.2, 146.6, 150.4, 151.4, 151.9, 152.1, 157.6, 159.3, 163.6, 167.0, 167.4, 170.0, 170.5, 173.3. MS (ESI+) *m/z*: 727; 729; 731 [MH]⁺; 749; 751; 753 [M+Na]⁺; ⁷⁹Br⁷⁹Br; ⁷⁹Br⁸¹Br; ⁸¹Br⁸¹Br; HRMS (ESI+) *m/z*: calcd for C₃₂H₃₂N₄NaO₆⁷⁹Br⁸¹Br: 751.0566 [M+Na]⁺; found 751.0531 [M+Na]⁺.

4.1.2.2. Methyl (S,E and S,Z)-2-acetamido-6-(2-{4-[5,7-dibromo-1-(4-methoxybenzyl)-2-oxoindolin-3-ylideneamino]phenyl}acetamido)hexanoate (4b). Red crystals (33.3 mg, 41%); mixture of *E* and *Z* isomers (*E/Z* 49:51); mp 99–101 °C; *R*_f 0.33 (silica, CHCl₃/MeOH 95:5). δ_{H} (500 MHz; CDCl₃): 1.21–1.82 (m, 12H), 1.98 (s, 3H), 2.02 (s, 3H), 3.17–3.27 (m, 4H), 3.57 (s, 2H), 3.62 (s, 2H), 3.71 (s, 3H), 3.73 (s, 3H), 3.76 (s, 3H), 3.78 (s, 3H), 4.51–4.58 (m, 2H), 5.27 (s, 2H), 5.43 (s, 2H), 5.65 (br s, 1H), 5.72 (br s, 1H), 6.23 (d, *J* = 8.0 Hz, 1H), 6.27 (d, *J* = 8.0 Hz, 1H), 6.80 (d, *J* = 1.5 Hz, 1H), 6.82 (d, *J* = 8.5 Hz, 2H), 6.85 (d, *J* = 8.0 Hz, 2H), 6.97 (d, *J* = 8.5 Hz, 2H), 7.11–7.15 (m, 4H), 7.22 (d, *J* = 9.0 Hz, 2H), 7.37 (d, *J* = 8.0 Hz, 2H), 7.40–7.46 (m, 2H), 7.59 (d, *J* = 1.5 Hz, 1H), 7.69 (s, 1H), 7.83 (d, *J* = 1.5 Hz, 1H). δ_{C} (126 MHz; CDCl₃): δ 22.5, 23.3, 23.4, 29.1, 30.0, 31.9, 32.2, 39.2, 39.3, 43.5, 43.7, 44.0, 44.6, 52.1, 52.6, 52.7, 55.5, 104.0, 104.7, 114.3, 114.4, 115.6, 116.7, 117.4, 118.2, 120.1, 121.1, 125.5, 126.2, 127.7, 128.2, 128.2, 128.5, 128.9, 129.9, 130.9, 132.3, 133.3, 141.0, 141.7, 142.1, 144.0, 148.6, 149.7, 151.9, 157.9, 159.3, 163.8, 170.4, 171.2, 171.4, 173.2. HRMS (ESI+) *m/z*: calcd for C₃₃H₃₅N₄O₆⁷⁹Br⁸¹Br: 743.0903 [MH]⁺; found 743.0888 [MH]⁺.

4.1.2.3. Methyl (S,E and S,Z)-2-acetamido-6-(3-{4-[5,7-dibromo-1-(4-methoxybenzyl)-2-oxoindolin-3-ylideneamino]phenyl}propanamido)hexanoate (4c). Red powder (111 mg, 70%); mixture of *E* and *Z* isomers (*E/Z* 55:45); mp 161–163 °C; *R*_f 0.42 (silica, DCM/MeOH 9:1); IR *v*_{max} 3288 (NH), 1734 (CO), 1638, 1558, 1446, 1296, 1251, 1180, 1137, 804, 721 cm^{−1}. δ_{H} (500 MHz; CDCl₃): 1.29–1.82 (m, 12H), 1.99 (s, 3H), 2.03 (s, 3H), 2.43–2.52 (m, 4H), 2.94–3.04 (m, 4H), 3.12–3.27 (m, 4H), 3.72 (s, 3H), 3.73 (s, 3H), 3.76 (s, 3H), 3.78 (s, 3H), 4.55 (t, *J* = 4.0 Hz, 2H), 5.27 (s, 2H), 5.43 (s, 2H), 5.62 (br s, 1H), 5.66 (br s, 1H), 6.32 (d, *J* = 6.0 Hz, 2H), 6.81 (d, *J* = 4.0 Hz, 2H), 6.83 (s, 1H), 6.85 (d, *J* = 8.5 Hz, 2H), 6.90 (d, *J* = 7.5 Hz, 2H), 7.10 (d, *J* = 8.0 Hz, 2H), 7.15 (d, *J* = 8.5 Hz, 2H), 7.21 (t, *J* = 7.5 Hz, 4H), 7.29 (d, *J* = 8.0 Hz, 2H), 7.58 (s, 1H), 7.68 (s, 1H), 7.85 (s, 1H). δ_{C} (126 MHz; CDCl₃): 22.5, 22.6, 23.3, 23.4, 28.9, 29.1, 31.6, 31.7, 32.1, 32.3, 38.6, 38.9, 39.0, 39.1, 43.9, 44.6, 52.0, 52.1, 52.6, 55.5, 103.8, 104.6, 114.3, 114.4, 115.6, 116.6, 117.9, 119.8, 121.2, 125.4, 126.5, 128.1, 128.2, 128.2, 128.6, 128.6, 128.8, 129.9, 139.4, 140.1, 140.7, 141.5, 141.9, 144.0, 146.2, 147.7, 149.2, 151.8, 157.9, 159.2, 159.3, 163.9, 169.5, 172.4, 172.6, 173.2. MS (ESI+) *m/z*: 755; 757; 759 [MH]⁺; ⁷⁹Br⁷⁹Br; ⁷⁹Br⁸¹Br; ⁸¹Br⁸¹Br; HRMS (ESI+) *m/z*: calcd for C₃₄H₃₆N₄NaO₆⁷⁹Br⁸¹Br: 779.0879 [M+Na]⁺; found 779.0896 [M+Na]⁺.

4.1.2.4. Methyl (S,E and S,Z)-2-acetamido-6-{3-[5,7-dibromo-1-(4-methoxybenzyl)-2-oxoindolin-3-ylideneamino]benzamido}hexanoate (4d). Orange crystals (83.4 mg, 78%); mixture of *E* and *Z* isomers (*E/Z* 47:53); mp 74–76 °C; *R*_f 0.56 (silica, CHCl₃/MeOH 95:5). IR *v*_{max} 3293 (NH), 1734 (CO), 1645, 1547, 1446, 1318, 1249, 1142, 801, 721 cm^{−1}. δ_{H} (500 MHz; CDCl₃): 1.36–1.91 (m, 12H), 1.97 (t, *J* = 7.0 Hz, 6H), 3.41–3.48 (m, 4H), 3.72

(s, 3H), 3.73 (s, 3H), 3.76 (s, 3H), 3.79 (s, 3H), 4.56–4.62 (m, 2H), 5.25 (s, 2H), 5.43 (s, 2H), 6.24 (d, $J = 7.5$ Hz, 1H), 6.28 (d, $J = 7.5$ Hz, 1H), 6.40 (t, $J = 5.5$ Hz, 1H), 6.55 (t, $J = 5.5$ Hz, 1H), 6.70 (d, $J = 1.5$ Hz, 1H), 6.82 (d, $J = 8.0$ Hz, 2H), 6.86 (d, $J = 8.5$ Hz, 2H), 7.08 (d, $J = 8.0$ Hz, 2H), 7.14 (d, $J = 9.0$ Hz, 2H), 7.21 (d, $J = 9.0$ Hz, 2H), 7.43 (t, $J = 8.0$ Hz, 1H), 7.46 (s, 1H), 7.53 (t, $J = 8.0$ Hz, 1H), 7.54 (d, $J = 1.5$ Hz, 1H), 7.59 (d, $J = 1.5$ Hz, 1H), 7.63 (d, $J = 8.0$ Hz, 1H), 7.70 (d, $J = 2.0$ Hz, 1H), 7.74 (d, $J = 7.5$ Hz, 1H), 7.83 (d, $J = 2.0$ Hz, 1H). δ_C (126 MHz; $CDCl_3$): 22.5, 22.6, 23.3, 23.4, 28.7, 29.0, 32.1, 32.4, 39.5, 39.8, 44.0, 44.6, 51.9, 52.0, 52.6, 52.7, 55.5, $^{104.0}$, $^{104.8}$, $^{114.3}$, $^{114.4}$, $^{115.8}$, $^{116.5}$, $^{116.7}$, $^{118.9}$, $^{120.1}$, $^{123.0}$, $^{124.7}$, $^{124.9}$, $^{125.6}$, $^{126.0}$, $^{126.9}$, $^{127.8}$, $^{128.1}$, $^{128.2}$, $^{128.3}$, $^{128.4}$, $^{129.1}$, $^{130.2}$, $^{135.4}$, $^{141.3}$, $^{141.9}$, $^{142.3}$, $^{144.1}$, $^{148.3}$, $^{149.7}$, $^{150.4}$, $^{152.3}$, $^{157.8}$, $^{159.2}$, $^{159.3}$, $^{163.6}$, $^{166.9}$, $^{167.5}$, $^{170.4}$, $^{170.5}$, $^{173.2}$.⁺ MS (ESI⁺) m/z : 727; 729; 731 [MH]⁺; $^{79}Br^{79}Br$; $^{79}Br^{81}Br$; $^{81}Br^{81}Br$. HRMS (ESI⁻) m/z : calcd for $C_{32}H_{31}N_4O_6^{79}Br^{81}Br$: 727.0590 [M-H]⁻; found 727.0380 [M-H]⁻.

4.1.2.5. Methyl (*S,E* and *S,Z*)-2-acetamido-6-(2-{3-[5,7-dibromo-1-(4-methoxybenzyl)-2-oxoindolin-3-ylideneamino]phenyl}acetamido)hexanoate (**4e**).

Red powder (98.5 mg, 82%); mixture of *E* and *Z* isomers (*E/Z* 37:63); mp 194–196 °C; R_f 0.44 (silica, DCM/MeOH 9:1). IR ν_{max} 3288 (NH), 1721 (CO), 1647, 1558, 1516, 1447, 1316, 1252, 1140, 720 cm^{-1} . δ_H (500 MHz; $CDCl_3$): δ 1.16–1.69 (m, 12H), 1.98 (s, 3H), 2.01 (s, 3H), 3.09 (m, 2H), 3.14–3.24 (m, 2H), 3.59 (s, 4H), 3.69 (s, 3H), 3.73 (s, 3H), 3.77 (s, 3H), 3.78 (s, 3H), 4.45 (d, $J = 3.5$ Hz, 1H), 4.53 (d, $J = 3.5$ Hz, 1H), 5.24 (s, 2H), 5.43 (s, 2H), 5.68 (br s, 1H), 5.91 (br s, 1H), 6.20–6.24 (m, 2H), 6.76 (s, 1H), 6.83 (d, $J = 8.0$ Hz, 4H), 6.91 (s, 2H), 7.03 (d, $J = 8.0$ Hz, 1H), 7.10 (d, $J = 8.5$ Hz, 4H), 7.21 (d, $J = 7.5$ Hz, 3H), 7.40 (t, $J = 8.0$ Hz, 1H), 7.45 (t, $J = 7.5$ Hz, 1H), 7.59 (s, 1H), 7.71 (s, 1H), 7.86 (s, 1H). δ_C (126 MHz; $CDCl_3$): 22.4, 22.5, 23.3, 23.4, 29.1, 29.9, 31.7, 32.1, 39.1, 39.4, 43.8, 44.0, 44.1, 44.6, 52.1, 52.3, 52.5, 52.6, 55.5, $^{104.1}$, $^{104.7}$, $^{114.4}$, $^{114.4}$, $^{115.8}$, $^{116.2}$, $^{116.9}$, $^{118.3}$, $^{119.4}$, $^{119.7}$, $^{120.4}$, $^{125.7}$, $^{126.0}$, $^{127.1}$, $^{127.7}$, $^{128.0}$, $^{128.2}$, $^{128.3}$, $^{128.5}$, $^{130.0}$, $^{130.5}$, $^{135.2}$, $^{137.3}$, $^{141.2}$, $^{141.8}$, $^{142.1}$, $^{144.1}$, $^{148.9}$, $^{150.1}$, $^{150.3}$, $^{152.0}$, $^{158.0}$, $^{159.3}$, $^{163.8}$, $^{170.3}$, $^{170.4}$, $^{170.7}$, $^{171.2}$, $^{173.2}$.⁺ MS (ESI⁺) m/z : 763; 765; 767 [M+Na]⁺; $^{79}Br^{79}Br$; $^{79}Br^{81}Br$; $^{81}Br^{81}Br$. HRMS (ESI⁻) m/z : calcd for $C_{33}H_{33}N_4O_6^{79}Br^{81}Br$: 741.0747 [M-H]⁻; found 741.0779 [M-H]⁻.

4.2. Hydrolysis studies

Hydrolysis studies were performed using a Varian Cary 500 Scan UV-vis-NIR spectrophotometer with 1 cm path length and disposable plastic cuvettes. Briefly, 9 μ mol of either **3a–e** or **4a–e** were dissolved in acetonitrile/water 98.5:1.5 (10 mL) to yield a stock solution of approximately 1 mM. Buffer solutions consisted of 1 M sodium acetate adjusted to pH 4.5 and pH 5.3 and 1 M HEPES adjusted to pH 7.4. The pH values of the solutions were measured using a pH Cube pH-mV-temp Meter (TPS, Springwood, Australia). The final reaction mixture in the cuvette consisted of stock solution/buffer/water in the ratio 1:2:2. All solutions were monitored kinetically at 435 nm for 4 h at either rt (23 °C) or 37 °C. The dependence of the absorption spectra (measured at $\lambda = 435$ nm) on time, expressed as A/A_0 versus t (where A = absorbance of the sample and A_0 = absorbance at time zero), was used to investigate the kinetics of imine hydrolysis, with all measurements performed on at least two independent occasions. The kinetic parameters k and $t_{1/2}$ were derived by nonlinear regression analysis of the $\ln(A/A_0)$ versus time plots using GraphPad Prism 5.00 (GraphPad Software, Inc., San Diego, CA, USA), with one-way, repeated measures ANOVA followed by a Tukey post-test to determine whether differences between data sets were significant, with significance set at $P < 0.05$.

Acknowledgments

We thank the University of Wollongong for financial support through the Centre for Medicinal Chemistry (CMC), the Centre for Medical Bioscience (CMB), a University of Wollongong Small Grant and a University Cancer Research Grant. An Australian Postgraduate Award to L. Matesic, a Cure Cancer Australia Foundation and Cancer Australia award to K. L. Vine, and a Cancer Institute New South Wales Fellowship to M. Ranson are also gratefully acknowledged.

Supplementary data

Supplementary data (hydrolysis graphs of imines **3a–e** vs their analogous imino lysines **4a–e** at pH 4.5 and hydrolysis graphs of imines **3a**, **3b** and **3d** at 23 °C vs 37 °C) associated with this article can be found, in the online version, at doi:10.1016/j.bmc.2011.01.015.

References and notes

- Garnett, M. C. *Adv. Drug Delivery Rev.* **2001**, *53*, 171–216.
- Chari, R. V. J. *Accounts Chem. Res.* **2008**, *41*, 98–107.
- Maxfield, F.; McGraw, T. *Nat. Rev. Mol. Cell Biol.* **2004**, *5*, 121–132.
- Kratz, F.; Beyer, U.; Schütte, M. T. *Crit. Rev. Ther. Drug Carrier Syst.* **1999**, *16*, 245–288.
- Allen, T. *Nat. Rev. Cancer* **2002**, *2*, 750–763.
- Etrych, T.; Jelinkova, M.; Rihova, B.; Ulbrich, K. J. *Controlled Release* **2001**, *73*, 89–102.
- Bae, Y.; Nishiyama, N.; Fukushima, S.; Koyama, H.; Yasuhiro, M.; Kataoka, K. *Bioconjugate Chem.* **2005**, *16*, 122–130.
- Bae, Y.; Fukushima, S.; Harada, A.; Kataoka, K. *Angew. Chem., Int. Ed.* **2003**, *42*, 4640–4643.
- Kale, A. A.; Torchilin, V. P. *Bioconjugate Chem.* **2007**, *18*, 363–370.
- Kakinoki, A.; Kaneo, Y.; Ikeda, Y.; Tanaka, T.; Fujita, K. *Biol. Pharm. Bull.* **2008**, *31*, 103–110.
- Kratz, F.; Müller, I. A.; Ryppa, C.; Warnecke, A. *ChemMedChem* **2008**, *3*, 20–53.
- Masson, C.; Garinot, M.; Mignet, N.; Wetzler, B.; Mailhe, P.; Scherman, D.; Bessodes, M. J. *Controlled Release* **2004**, *99*, 423–434.
- Kong, S. D.; Luong, A.; Manorek, G.; Howell, S. B.; Yang, J. *Bioconjugate Chem.* **2007**, *18*, 293–296.
- Ulbrich, K.; Subr, V. *Adv. Drug Delivery Rev.* **2004**, *56*, 1023–1050.
- Dubowchik, G. M.; Walker, M. A. *Pharmacol. Ther.* **1999**, *83*, 67–123.
- Alley, S. C.; Benjamin, D. R.; Jeffrey, S. C.; Okeley, N. M.; Meyer, D. L.; Sanderson, R. J.; Senter, P. D. *Bioconjugate Chem.* **2008**, *19*, 759–765.
- Kaneko, T.; Willner, D.; Monkovic, I.; Knipe, P. O.; Braslawsky, G. R.; Greenfield, R. S.; Vyas, D. M. *Bioconjugate Chem.* **1991**, *2*, 133–141.
- Gillies, E. R.; Goodwin, A. P.; Fréchet, J. M. J. *Bioconjugate Chem.* **2004**, *15*, 1254–1263.
- Jain, R.; Standley, S. M.; Fréchet, J. M. J. *Macromolecules* **2007**, *40*, 452–457.
- Kalia, J.; Raines, R. T. *Angew. Chem., Int. Ed.* **2008**, *47*, 7523–7526.
- Kim, Y. H.; Park, J. H.; Lee, M.; Kim, Y.-H.; Park, T. G.; Kim, S. W. J. *Controlled Release* **2005**, *103*, 209–219.
- Singh, Y.; Palombo, M.; Sinko, P. J. *Curr. Med. Chem.* **2008**, *15*, 1802–1826.
- Vine, K. L.; Locke, J. M.; Ranson, M.; Benkendoff, K.; Pyne, S. G.; Bremner, J. B. *Bioorg. Med. Chem.* **2007**, *15*, 931–938.
- Vine, K. L.; Locke, J. M.; Ranson, M.; Pyne, S. G.; Bremner, J. B. *J. Med. Chem.* **2007**, *50*, 5109–5117.
- Matesic, L.; Locke, J. M.; Bremner, J. B.; Pyne, S. G.; Skropeta, D.; Ranson, M.; Vine, K. L. *Bioorg. Med. Chem.* **2008**, *16*, 3118–3124.
- Lemieux, G. A.; Bertozzi, C. R. *Trends Biotechnol.* **1998**, *16*, 506–513.
- Ding, C.; Gu, J.; Qu, X.; Yang, Z. *Bioconjugate Chem.* **2009**, *20*, 1163–1170.
- Sedlak, M.; Pravda, M.; Staud, F.; Kubcová, L.; Tycová, K.; Ventura, K. *Bioorg. Med. Chem.* **2007**, *15*, 4069–4076.
- Sedlak, M.; Pravda, M.; Kubcová, L.; Mikulcuková, P.; Ventura, K. *Bioorg. Med. Chem. Lett.* **2007**, *17*, 2554–2557.
- Gu, J.; Cheng, W.-P.; Liu, J.; Lo, S.-Y.; Smith, D.; Qu, X.; Yang, Z. *Biomacromolecules* **2008**, *9*, 255–262.
- Muller, I. A.; Kratz, F.; Jung, M.; Warnecke, A. *Tetrahedron Lett.* **2010**, *51*, 4371–4374.
- Konkel, M. J.; Lagu, B.; Boteju, L. M.; Jimenez, H.; Noble, S.; Walker, M. W.; Chandrasena, G.; Blackburn, T. P.; Nikam, S. S.; Wright, J. L.; Kornberg, B. E.; Gregory, T.; Pugsley, T. A.; Akunne, H.; Zoski, K.; Wise, L. D. *J. Med. Chem.* **2006**, *49*, 3757–3758.
- Abadi, A. H.; Abou-Seri, S. M.; Abdel-Rahman, D. E.; Klein, C.; Lozach, O.; Meijer, L. *Eur. J. Med. Chem.* **2006**, *41*, 296–305.
- Nozaki, S. *J. Peptide Sci.* **2006**, *12*, 147–153.
- Han, S.-Y.; Kim, Y.-A. *Tetrahedron* **2004**, *60*, 2447–2467.

36. Kalavska, D.; Kalavsky, S.; Kosturiak, A.; Szalo, A. *Chem. Zvesti* **1978**, *32*, 650–657.
37. Smith, M. B.; March, J. *March's Advanced Organic Chemistry: Reactions, Mechanism, and Structure*, 6th ed.; John Wiley & Sons: New York, USA, 2007.
38. Laube, T.; Ha, T. K. *J. Am. Chem. Soc.* **1988**, *110*, 5511–5517.
39. Baker, M. A.; Gray, B. D.; OhlssonWilhelm, B. M.; Carpenter, D. C.; Muirhead, K. *A. J. Controlled Release* **1996**, *40*, 89–100.
40. Nakagawa-Goto, K.; Nakamura, S.; Bastow, K. F.; Nyarko, A.; Peng, C.-Y.; Lee, F.-Y.; Lee, F.-C.; Lee, K.-H. *Bioorg. Med. Chem. Lett.* **2007**, *17*, 2894–2898.
41. Still, W. C.; Kahn, M.; Mitra, A. *J. Org. Chem.* **1978**, *43*, 2923–2925.